Relative Patterns and Rates of Evolution in Heron Nuclear and Mitochondrial DNA

Frederick H. Sheldon, Clare E. Jones,* and Kevin G. McCracken†*

*Museum of Natural Science and †School of Forestry, Wildlife, and Fisheries, Louisiana State University at Baton Rouge

Mitochondrial cytochrome *b* sequence data from 15 species of herons (Aves: Ardeidae), representing 13 genera, were compared with DNA hybridization data of single-copy nuclear DNA (scnDNA) from the same species in a taxonomic congruence assessment of heron phylogeny. The two data sets produced a partially resolved, completely congruent estimate of phylogeny with the following basic structure: (*Tigrisoma, Cochlearius,* (((*Zebrilus,* (*Ixobrychus, Botaurus*)), (((*Ardea, Casmerodius*), *Bubulcus*), ((*Egretta thula, Egretta caerulea, Egretta tricolor*), *Syrigma*), *Butorides, Nycticorax, Nyctanassa*)))). Because congruence indicated similar phylogenetic information in the two data sets, we used the relatively unsaturated DNA hybridization distances as surrogates of time to examine graphically the patterns and rates of change in cytochrome *b* distances. Cytochrome *b* distances were computed either from whole sequences or from partitioned sequences consisting of transitions, transversions, specific codon site positions, or specific protein-coding regions. These graphical comparisons indicated that unpartitioned cytochrome *b* has evolved at 5–10 times the rate of scnDNA. Third-position transversions appeared to offer the most useful sequence partition for phylogenetic analysis because of their relatively fast rate of substitution (two times that of scnDNA) and negligible saturation. We also examined lineage-based rates of evolution by comparing branch length patterns between the nuclear and cytochrome *b* trees. The degree of correlation in corresponding branch lengths between cytochrome *b* and DNA hybridization trees depended on DNA sequence partitioning. When cytochrome *b* sequences were not partitioned, branch lengths in the cytochrome *b* and DNA hybridization trees were not correlated. However, when cytochrome *b* sequences were reduced to third-position transversions (i.e., unsaturated, relatively fast changing data), branch lengths were correlated. This finding suggests that lineage-based rates of DNA evolution in nuclear and mitochondrial genomes are influenced by common causes.

Introduction

The herons (Aves: Ardeidae) offer an excellent opportunity to examine patterns and rates of evolution in mitochondrial DNA (mtDNA) genes. DNA hybridization comparisons of heron single-copy nuclear DNA (scnDNA) indicate that the major clades of herons—bitterns, tiger herons, boat-billed heron, and day and night herons—have evolved at different rates from one another (fig. 1). These rate differences are slight but consistent among groups. For example, bittern scnDNAs have evolved about 25% faster than day and night heron scnDNAs, and boat-bill and tiger heron scnDNAs have evolved about 19% more slowly than those of day and night herons. The existence of these lineage-based rate differences in scnDNA raises the question of whether mtDNA displays the same rate pattern. Similarity in lineage-based rates of evolutionary change between nuclear and mitochondrial DNAs might not be expected, because the two genomes are unlinked and display different overall rates (e.g., Avise 1994, p. 103). However, comparisons among older groups of vertebrates suggest that nuclear and mitochondrial DNA evolutionary rates may, in fact, covary (Martin and Palumbi 1993; Mindell et al. 1996; Martin 1999). The herons offer an opportunity to determine whether covariation occurs in closely related birds.

The nuclear DNA hybridization data also provide a useful perspective on patterns and rates of mtDNA evolution via rate graphs (e.g., Brown, George, and Wilson 1979). Analyses of DNA hybridization data suggest that even the longest heron scnDNA distances are not compressed by saturation due to multiple mutations at single-base sites (Sheldon and Bledsoe 1989). Thus, heron scnDNA distances provide a fairly linear, relative timescale that allows examination of genetic distances derived from mtDNA sequence data (although the scnDNA scale is admittedly perturbed by variable lineage-based rates). The use of scnDNA to obtain a relative timescale presents an advantage over the usual relative method of examining mtDNA rate patterns, i.e., comparing partitioned versus complete sequence (unpartitioned) distances (e.g., Hackett 1996; Nunn and Cracraft 1996; Griffiths 1997). For example, the relative pattern of transversional change through time is generally visualized by plotting distances based on transversions versus a timescale (on the x-axis) consisting of distances based on all of the sequence data. The complete sequence distances are usually corrected for back mutations using a distance model, such as the Kimura three-parameter method (Kimura 1981), to increase their linearity with time. However, a timescale based on complete sequences presents at least two problems: (1) partitioned distances are not independent of complete sequence distances; they are subsets (Edwards 1997), and (2) only partitioned sequence data, not the complete sequences, may be examined for patterns of change, because there is no way of obtaining a relative time perspective for distances based on compete sequences. Using DNA hybridization distances as the timescale provides an independent view of divergence patterns for both partitioned and complete mtDNA sequences. This independent perspective permits assessments of the interdependence between partitioned and complete se-

Key words: Ardeidae, congruence analysis, cytochrome *b* sequence, DNA-DNA hybridization, phylogeny, rates of evolution.

Address for correspondence and reprints: Frederick H. Sheldon, Museum of Natural Science, 119 Foster Hall, Louisiana State University, Baton Rouge, Louisiana 70803. E-mail: fsheld@lsu.edu.

Mol. Biol. Evol. 17(3):437–450. 2000

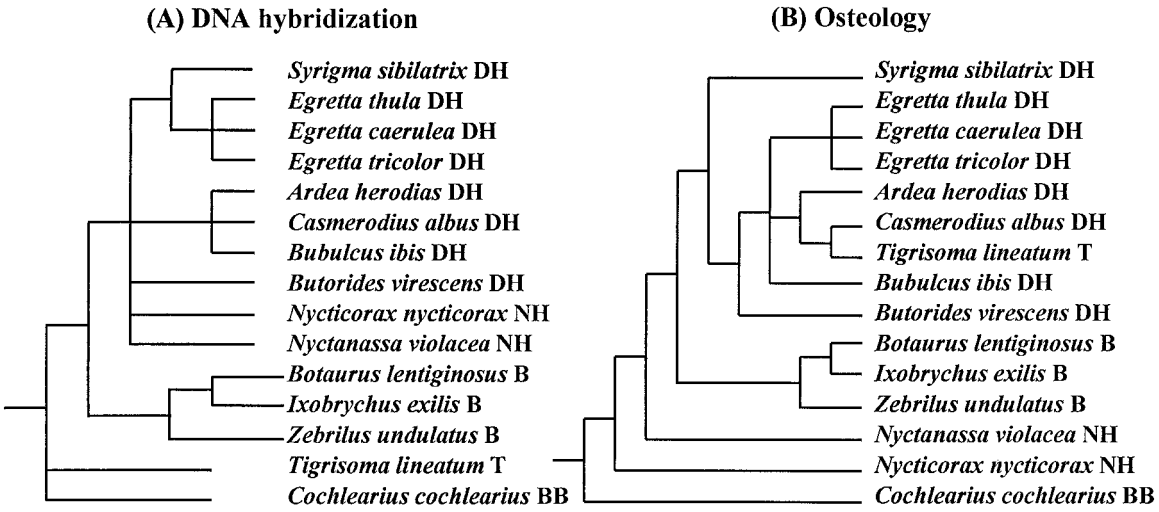

FIG. 1.—Previous estimates of heron phylogeny. *A*, DNA hybridization tree based on distances fitted to branching patterns by unweighted least-squares (PHYLIP's Fitch program; Felsenstein 1989). This tree conforms to the jackknife strict-consensus tree of Sheldon (1987*b*), with the following caveats: *Egretta caerulea* was added by hand based on an incomplete comparison matrix (Sheldon 1987*b*); the position of *Zebrilus undulatus* was determined using a small matrix consisting of *Egretta thula*, *Ixobrychus exilis*, *Cochlearius cochlearius*, *Tigrisoma lineatum*, and *Tigriornis leucolophus* (Sheldon, McCracken, and Stuebing 1995); the multifurcation at the base of the tree reflects disagreement between the jackknife analysis of Sheldon (1987*b*) and the bootstrap analysis of Sheldon, McCracken, and Stuebing (1995); and differences in branch lengths for various groups, discussed by Sheldon (1987*a*) and Sheldon and Kinnarney (1993), are represented schematically. *B*, Osteological estimate of heron phylogeny (McCracken and Sheldon 1998). This tree is based on an unweighted parsimony analysis of the 33 skeletal characters of Payne and Risley (1976) and is extracted from a 50% majority-rule consensus of 2,500 most-parsimonious trees of 50 herons and 9 ciconiiform outgroups (McCracken and Sheldon 1998). The two letters after each name designate the heron's ecological group: DH = day herons, NH = night herons, B = bitterns, T = tiger herons, BB = boat-billed heron.

quence data and the effectiveness of various methods of correcting complete-sequence distances for back mutations.

These analyses of lineage-based rates and partition divergence patterns assume that DNA hybridization measures mainly scnDNA differences among species, with the bulk of repetitive DNA having been removed and the influence of mtDNA overwhelmed by the much larger nuclear genome. Thus, a DNA-DNA hybridization distance theoretically reflects an average of a wide range of scnDNA divergences between two species and not that of a small, perhaps aberrantly evolving, portion of the nuclear genome or mtDNA. As best we can tell from analyses of the DNA hybridization technique (e.g., Britten, Graham, and Neufeld 1974), congruence among phylogenetic trees (e.g., Bledsoe and Raikow 1990; Sheldon, Whittingham, and Winkler 1999), and the behavior of DNA hybridization in a phylogenetic context or under perturbation (e.g., Bleiweiss and Kirsch 1992; Sheldon and Kinnarney 1993), this assumption is valid.

In this paper, we use uncorrected heron scnDNA hybridization distances to assess patterns and rates of heron mitochondrial cytochrome *b* gene sequence evolution. The nuclear and mitochondrial DNA data were compared in two ways, as discussed above. First, cytochrome *b* sequences were subdivided by codon and protein region positions into as many as 18 partitions. Genetic distances between pairs of species then were computed from these partitions and plotted against DNA hybridization distances to permit a graphical comparison of divergence patterns. Second, we examined lineage-based rates of molecular evolution. These comparisons were possible because the two data sets yielded congruent estimates of heron phylogeny. Phenetic and patristic (branch length) distances in both data sets were examined via relative-rate tests (Sarich and Wilson 1967), and the correlation of lineage-based rates between the cytochrome *b* and DNA hybridization trees was tested by the method of Omland (1994, 1997).

The comparison of scnDNA hybridization and cytochrome *b* sequence data also provided a taxonomic congruence assessment of heron phylogeny. Until now, there have been only two modern phylogenetic studies of herons: DNA hybridization studies (Sheldon 1987*b*; Sheldon and Kinnarney 1993; and Sheldon, McCracken, and Stuebing 1995) and a cladistic analysis of osteological characters (Payne and Risley 1976). These two data sets yielded fundamentally different estimates of heron phylogeny (fig. 1), but it was unclear which estimate was better. The cytochrome *b* sequence analysis breaks this log jam and shows via phylogenetic congruence (Bledsoe and Raikow 1990) that the DNA hybridization tree is probably more accurate than the cladogram derived from osteological characters. The cytochrome *b* data also help to resolve some relationships that were unclear in the DNA hybridization tree.

Materials and Methods

Selection of Taxa

Species whose cytochrome *b* genes were sequenced in this study are listed in table 1. They include 15 herons, representing 13 of the 20 genera in the family, and an outgroup, glossy ibis (*Plegadis falcinellus*). We also

Table 1
Species Whose Cytochrome *b* Genes were Sequenced for this Study

Species Name	Common Name	Sample No.[a]	Collection Locality	GenBank Accession No.
Syrigma sibilatrix	Whistling heron	B6613	Bolivia	AF193820
Ardea herodias	Great blue heron	B4095	Louisiana	AF193821
Casmerodius albus	Great egret	B1343	Louisiana	AF193822
Bubulcus ibis	Cattle egret	B19756	Louisiana	AF193823
Egretta tricolor[b]	Tricolored heron	B19408	Louisiana	AF193824
Egretta caerulea	Little blue heron	B5283	Louisiana	AF193825
Egretta thula	Snowy egret	B6385	Louisiana	AF193826
Butorides virescens	Green heron	B108578	Louisiana	AF193827
Nyctanassa violacea	Yellow-crowned night heron	B15549	Louisiana	AF193828
Nycticorax nycticorax	Black-crowned night heron	B18955	Audubon Zoo	AF193829
Cochlearius cochlearius	Boat-billed heron	B1339	Audubon Zoo	AF193830
Tigrisoma lineatum	Rufescent tiger heron	B12256	Bolivia	AF193831
Ixobrychus exilis	Least bittern	B3882	Louisiana	AF193832
Botaurus lentiginosus	American bittern	B18981	Louisiana	AF193833
Zebrilus undulatus[b]	Zigzag heron	B12873	Bolivia	AF193834
Plegadis falcinellus	Glossy ibis	B5273	Louisiana	AF193819

[a] Louisiana State Museum of Natural Science catalog numbers.

[b] Species not compared in a complete DNA hybridization matrix by Sheldon (1987*b*). *Egretta tricolor* was compared with most, but not all, of the species studied by Sheldon (1987*b*). *Zebrilus undulatus* was compared by DNA hybridization with some other herons by Sheldon, McCracken, and Stuebing (1995).

obtained outgroup sequences from GenBank as follows: hamerkop (*Scopus umbretta*), U08936; African spoonbill (*Platalea alba*), U08941; shoebill (*Balaeniceps rex*), U08937; black vulture (*Coragyps atratus*), U08946; and wood stork (*Mycteria americana*), U72779. These outgroups are among the herons' closest known relatives (Sibley and Ahlquist 1990). As a more distant outgroup, we used the domestic chicken (*Gallus domesticus*), NC001323 (Desjardins and Morais 1990). These outgroups were used in all tree reconstructions and relative-rate tests.

We sequenced the cytochrome *b* genes of these particular heron species because they had been compared previously by DNA hybridization (fig. 1*A*). Thirteen of the heron species were compared in a complete DNA-DNA hybridization matrix (Sheldon 1987*b*). The tricolored heron (*Egretta tricolor*) was compared with most, but not all, of the 13 other species in that study. The zigzag heron (*Zebrilus undulatus*) was compared with representative species of the main heron clades by Sheldon, McCracken, and Stuebing (1995).

Cytochrome *b* Sequencing

To minimize contamination of the mitochondrial cytochrome *b* sequences with paralogous nuclear pseudogenes (Quinn 1997), we used relatively mtDNA-rich tissues as sources of DNA, rather than blood samples, which have relatively low mtDNA copy numbers (Sorenson and Fleischer 1996). We also amplified the entire cytochrome *b* gene as a single piece, rather than in smaller sections, to help reduce the chance of amplifying nuclear pseudogenes. Possible pseudogene contamination was also checked by partition analysis to see if the sequences exhibited pseudogene properties (stop codons, equal rates in all codon site positions, lack of domain-specific amino acid conservation, etc.).

Genomic DNA was isolated from 0.1 g of heart, liver, or muscle tissue using standard phenol/chloroform extraction (Hillis et al. 1990). Most of the mitochondrial cytochrome *b* gene and part of the adjacent threonine tRNA gene (chicken mtDNA genome positions 14991–16063; Desjardins and Morais 1990) were amplified by the polymerase chain reaction (PCR) from total genomic DNA preparations using a combination of bird-specific and heron-specific primers. The gene was amplified as a single continuous fragment using the primer pair L14990 (5′-CCATCCAACATCTCAGCATGATGAAA-3′) (Kocher et al. 1989) and H16064 (5′-GGAGTCTT-CAGTCTCTGGTTTACAAGACC-3′) (Helm-Bychowski and Cracraft 1993). Numbers in the primer names refer to the 3′ base positions of the primers as referenced to the chicken mtDNA sequence (Desjardins and Morais 1990). ''L'' and ''H'' refer to heavy- and light-strand primers. PCR reactions were carried out in a GeneAmp PCR System 2400 oil-free thermocycler (Perkin Elmer Applied Biosystems, Norwalk, Conn.), using a 50-μl reaction volume containing 0.5 μM of each primer, 10 mM of each dNTPs, 2.5 mM $MgCl_2$, and 1.25 U *Taq* polymerase (Perkin Elmer). Thermal cycling was as follows: 35 cycles with denaturation at 94°C for 30 s, annealing at 52°C for 30 s, and extension at 72°C for 30 s. These cycles were followed by a final extension at 72°C for 7 min.

PCR products were electrophoresed in 1% agarose gel at 110 V for 1 h, stained with 10 μg/μl ethidium bromide, excised, and purified using GeneClean II (BIO-101, La Jolla, Calif.) and QIAquick Gel Extraction Kits (QIAGEN, Santa Clarita, Calif.). Both strands of the PCR product were sequenced using various combinations of the primers noted above and the following internal primers: (1) L15320 (5′-GGATACGTCCT-ACCATGAGGACAAATATCCTTCTGAGG-3′), (2) H15425 (5′-GGAGGAAGTGTAAAGCGAAGAATC-3′), (3) H15710 (5′-GTAGGCGAATAGGAAGTATC-3′), and (4) L15656 (5′-AACCTACTAGGAGACCCA-GA-3′). We developed the first two primers, and the

latter two are from Helm-Bychowski and Cracraft (1993). For manual sequencing, we performed chain termination sequencing (Sanger, Nicklen, and Coulson 1977) with a 70170 Sequenase PCR Product sequencing kit (Amersham/UB, Cleveland, Ohio). Sequencing products were electrophoresed through a 6% polyacrylamide gel and visualized by autoradiography. For automated sequencing, we used a BigDye Terminator Cycle Sequencing Kit (Perkin Elmer Applied Biosystems), followed by sequencing in an ABI 377 automated sequencer (Perkin Elmer Applied Biosystems) with a 5% Long Ranger (FMC) gel. Light- and heavy-strand sequences that were obtained manually were scored visually, whereas those collected from the ABI 377 were scored using Sequencher 3.1 (Gene Codes Corporation, Ann Arbor, Mich.). The newly generated cytochrome *b* sequences have been deposited in GenBank; accession numbers are listed in table 1.

Data Analysis

The heron cytochrome *b* sequences were aligned by eye relative to the chicken sequence (Desjardins and Morais 1990) using editing and translation features in MEGA (Kumar, Tamura, and Nei 1993). Base frequencies, site variation, transition and transversion values, and some distance values also were determined with MEGA. Parsimony and maximum-likelihood trees were constructed and bootstrap analysis was performed with PAUP*, version 4.0b1 (Swofford 1998). The appropriate minimum-parameter, maximum-likelihood model was determined by likelihood ratio tests of the sequence data optimized on a neighbor-joining tree via Model Test 2.0 (Posada and Crandall 1998). The most appropriate model appeared to be the Kimura (1981) three-parameter model (K3P), with adjustments for unequal nucleotide frequencies and site-specific rate differences (K3Puf + gamma). Distance values used in tree-building were computed by PAUP*, and distance trees were constructed by least-squares using PHYLIP, version 3.5c (Felsenstein 1995). Alternative tree branching patterns were constructed with MacClade (Maddison and Maddison 1992).

To partition the cytochrome *b* sequence data, we followed the logic of Griffiths (1997). The data were partitioned as transitions and transversions according to (1) codon position and (2) protein region and codon position. The first division resulted in six partitions (three codon positions $\times$ two states [transition or transversion]). The second division resulted in 18 partitions (three codon positions $\times$ two states $\times$ three protein regions). The protein regions were the matrix, transmembrane, and intermembrane regions as defined by Zhang et al. (1998). Each partition of the data was graphed as uncorrected percentage of difference (MEGA's p-distance) versus DNA hybridization distance (uncorrected Tm, as defined by Sheldon and Bledsoe 1989). To estimate the instantaneous transition : transversion ratio (Ti/Tv), we used three methods. Ti/Tv was measured as the steepest slope of Ti/Tv plotted against DNA hybridization distance, as the steepest slope of transitional distances plotted against transversional distances (Hasegawa, Kishino, and Yano 1985; Moore and DeFilippis 1997), and from the maximum-likelihood rate parameters estimated by PAUP*.

Trees were inferred from cytochrome *b* sequences, without reference to the DNA hybridization data, by the following methods: (1) weighted parsimony, (2) maximum-likelihood using the K3Puf + gamma model (transition rate = 6.082, A$\leftrightarrow$C and G$\leftrightarrow$T = 1, A$\leftrightarrow$T and G$\leftrightarrow$C = 0.4858, α = 0.2698), and (3) least-squares fitting of K3Puf and K3Puf + gamma distances. Trees were also inferred using sequence partitions that exhibited the most linear distance-to-''time'' relationship when DNA hybridization distances were used to estimate time. Searches for best trees were heuristic and consisted of 100 parsimony or 20 maximum-likelihood randomized efforts with TBR branch-swapping and MULPARS options in effect. Fifty percent majority-rule bootstrap trees were built from 100 pseudoreplicates. The significance of differences in branching patterns between the best DNA hybridization topology and the most parsimonious or maximum-likelihood cytochrome *b* trees were determined via the Kishino-Hasegawa test (Kishino and Hasegawa 1989) implemented in PAUP*.

Rates of cytochrome *b* evolution were examined using a relative-rate test (Sarich and Wilson 1967) consisting of Friedman repeated-measures ANOVA on ranks, followed by Student-Newman-Keuls pairwise comparisons (Houde 1987). Distances from each of the seven outgroups to each heron species were compared. We tested phenetic distances (uncorrected proportional distances) and patristic distances (tree length distances) for a variety of data partitions. We used relative-rate tests to determine rate variation, instead of likelihood ratio (e.g., Sorhannus and Van Bell 1999) or other tree-based tests (e.g., Felsenstein 1984), because relative-rate tests indicate specifically which lineages differ in rates and by how much they differ.

Lineage-based rates of molecular evolution were compared between cytochrome *b* and DNA hybridization trees using the total-evolution method of Omland (1997). To perform this test, we used the DNA hybridization tree, which was congruent with cytochrome *b* trees based on bootstrap support, and then (1) optimized the DNA hybridization and cytochrome *b* distances and characters on this topology by least-squares and maximum-likelihood, respectively; (2) determined the total length of each lineage from heron ingroup node to branch tip (=''total evolution''); and (3) computed contrasts (differences) between pairs of total-evolution values as described by Omland (1997). To determine whether the contrasts needed to be corrected for a node-density effect, i.e., a bias in which rate of evolution is directly correlated with number of tree nodes (Fitch and Bruschi 1987), we first plotted total evolution as a function of number of nodes. The final contrasts were either positive or negative in sign. The degree to which contrasts agreed in signs between trees was determined and tested using a nonparametric binomial test, with the null hypothesis that 50% of the signs would agree by chance.

Table 2
Summary of Heron Cytochrome *b* Sequence Variability by Protein Regions

All Positions	Matrix	Transmembrane	Intermembrane
DNA Sequences			
1,041 nt	99 nt	627 nt	315 nt
408 variable sites	38 variable sites	265 variable sites	105 variable sites
39% variable sites	38% variable sites	42% variable sites	33% variable sites
256 informative sites	24 informative sites	160 informative sites	72 informative sites
25% informative sites	24% informative sites	26% informative sites	23% informative sites
Protein sequences			
347 amino acids	33 amino acids	209 amino acids	105 amino acids
69 variable sites	9 variable sites	44 variable sites	16 variable sites
20% variable sites	27% variable sites	21% variable sites	15% variable sites
24 informative sites	4 informative sites	17 informative sites	3 informative sites
7% informative sites	12% informative sites	8% informative sites	3% informative sites

NOTE.—Protein regions defined by Zhang et al. (1998). Informative sites are those in which character states are potentially informative for parsimony analysis.

Results

Partition Analysis and Characteristics of the Cytochrome *b* Data

The length of the cytochrome *b* gene sequenced in this study was 1041 bp. The sequence corresponds to positions 14992–16034 of the chicken mtDNA genome (Dejardins and Morais 1990). Average nucleotide composition of the heron sequences is as follows: adenine, 27.6%; thymine, 24.6%; cytosine, 34.9%; and guanine, 12.8%. Nucleotide composition is fairly even at first codon positions: A, 25.4%; T, 22.2%; C, 30.2%; and G, 22.2%. At second positions, thymine is prevalent and guanine is reduced: A, 19.8%; T, 40.4%; C, 26.6%; and G, 13.3%. At third positions, adenine and cytosine are prevalent and thymine and guanine are reduced: A, 37.6%; T, 11.2%; C, 48.1%; and G, 3.1%. This pattern is normal for the bird mitochondrial cytochrome *b* gene (e.g., Edwards, Arctander, and Wilson 1991; Nunn and Cracraft 1996; Slikas 1997). Variation among nucleotide sites of the heron cytochrome *b* sequences is summarized in table 2. Of 408 variable sites, 77 (19%) are located in first codon positions, 32 (8%) are located in second positions, and 299 (73%) are located in third positions. Of 256 potentially parsimony-informative sites, 31 (12%) are in first codon positions, 15 (6%) are in second positions, and 210 (82%) are in third positions. For the three protein regions (table 2), the largest percentage of variable nucleotide sites occurs in the transmembrane region, with the matrix being the next most variable and the intermembrane being the least variable. For amino acid variation, the pattern of percentages changes, such that the matrix region is more variable than the transmembrane region, and the transmembrane region is more variable than the intermembrane region. The significance of this pattern of amino acid variation is difficult to judge, because of the small number of matrix sites compared with intermembrane and transmembrane sites. The conservation of intermembrane amino acids, in particular, is expected because of the presence of many active site residues in this part of the protein (Degli Esposti et al. 1993; Zhang et al. 1998).

Cytochrome *b* and DNA hybridization distances between species are listed in table 3 and graphed in figure 2. It appears that the initial rate of cytochrome *b* DNA evolution is about 5–10 times as fast as the scnDNA rate, assuming a DNA hybridization distance of ΔTm 1 $\cong$ 1% DNA divergence (Springer, Davidson, and Britten 1992). Uncorrected heron cytochrome *b* divergences range from 5% (*E. tricolor* to *Egretta caerulea*) to 16% (*Tigrisoma* to *Botaurus*), with most lying between 11% and 14%. Correction for back mutations in the cytochrome *b* data using the K3Puf method (fig. 2) increases distances but does not reduce the flattening of the right-hand side of the curve that signals saturation. The saturation effect is reduced, however, if the K3Puf distances are further corrected for site-specific rate differences using the gamma-distribution approach (fig. 2). However, the addition of the gamma-distribution parameter causes an expected increase in the variance of the distance values (Swofford et al. 1996).

Graphical comparisons of uncorrected distances computed from cytochrome *b* sequences partitioned by codon site positions, transitions, and transversions are presented in figure 3. As is commonly found (e.g., Irwin, Kocher, and Wilson 1991; Hackett 1996; Griffiths 1997), third-position transversions display the most promising pattern in terms of phylogenetic reconstruction: a steep and largely linear divergence pattern in relationship to time. They appear to diverge at about twice the rate of DNA hybridization distances, assuming ΔTm 1 $\cong$ 1% DNA divergence. First-position transitions and transversions and second-position transitions increase with time (especially for ingroup comparisons), but without pronounced slopes. Second-position transversions do not increase appreciably with time, and third-position transitions appear heavily saturated, except for distances among closely related species (e.g., egret species).

Graphical comparisons of the data partitioned by protein regions, codon site positions, transitions, and transversions are presented in figure 4. The most linear patterns involve third-position transversions in the transmembrane (fig. 4*A*) and intermembrane (fig. 4*B*) regions and first-position transitions in the transmembrane re-

Table 3
Cytochrome *b* Proportional Distances (Upper Right) Versus DNA Hybridization ΔTm Values[a] (Lower Left)

	1	2	3	4	5	6	7	8	9	10	11	12	13	14	15	16
1. *Syrigma*		0.111	0.121	0.123	0.096	0.095	0.097	0.118	0.124	0.112	0.128	0.147	0.122	0.127	0.118	0.157
2. *Ardea*	3.79		0.080	0.108	0.111	0.116	0.112	0.114	0.119	0.117	0.121	0.147	0.125	0.117	0.119	0.144
3. *Casmerodius*	3.70	1.60		0.101	0.112	0.118	0.118	0.124	0.112	0.108	0.138	0.157	0.147	0.133	0.135	0.146
4. *Bubulcus*	3.55	1.83	1.50		0.111	0.118	0.119	0.132	0.138	0.126	0.133	0.148	0.126	0.128	0.135	0.161
5. *tricolor*		3.90	3.20	3.60		0.050	0.061	0.109	0.111	0.104	0.120	0.138	0.114	0.111	0.117	0.150
6. *Egretta caerulea*	2.80	3.20	3.38	3.60	1.30		0.055	0.108	0.104	0.105	0.115	0.139	0.111	0.114	0.117	0.147
7. *Egretta thula*	2.88	3.83	3.63	3.89	1.20	1.33		0.111	0.113	0.106	0.118	0.137	0.117	0.117	0.113	0.143
8. *Butorides*	3.94	3.51	3.30	3.32	4.00	3.90	3.99		0.131	0.121	0.141	0.152	0.120	0.124	0.131	0.160
9. *Nyctanassa*	4.00	3.46	3.23	3.35		3.80	3.85	3.59		0.112	0.137	0.155	0.135	0.126	0.124	0.159
10. *Nycticorax*	3.72	3.53	3.30	3.36	4.00	3.95	3.91	3.77	3.34		0.120	0.150	0.125	0.122	0.125	0.155
11. *Cochlearius*	5.80	5.71	5.30	5.60		6.40	5.98	5.80	5.50	5.64		0.141	0.125	0.137	0.134	0.155
12. *Tigrisoma*	6.02	5.93	5.71	5.74	6.20	5.80	6.10	5.93	5.84	5.84	4.90		0.148	0.156	0.139	0.164
13. *Ixobrychus*	5.76	5.78	5.50	5.66		5.60	6.00	5.80	5.75	5.60	7.00	6.78		0.087	0.111	0.165
14. *Botaurus*	5.70	6.10	5.80	5.80	6.30	6.10	5.90	6.00	5.70	5.70	6.90	6.60	2.60		0.119	0.159
15. *Zebrilus*							4.60				5.50	5.75	4.36			0.147
16. *Plegadis*	10.12	9.96	10.10	10.06		10.00	10.41	10.10	10.40	10.17	9.66	9.46	10.90	10.80	9.65	

[a] DNA hybridization distances are averages of replicate and reciprocal measurements (Sheldon 1987*b*).

FIG. 2.—Cytochrome *b* sequence distances versus DNA hybridization distances. Closed circles represent uncorrected proportional distances, open circles represent Kimura (1981) three-parameter distances with empirical base frequencies (K3Puf), and closed squares represent K3Puf distances with gamma-distribution rate correction ($\alpha = 0.26$).

gion (fig. 4*E*). Third-position matrix transversions (fig. 4*C*), first-position transmembrane transversions (fig. 4*D*), and second-position transmembrane transitions (fig. 4*F*) also appeared to increase with DNA hybridization divergence, but with greater scatter of points. Other partitions (not shown) did not display an increase of divergence with relative time. Figure 4*C* shows distinct horizontal groups of points, but these are simply an artifact of the small number of sites in the matrix region. Most of the apparent nucleotide change occurred in the transmembrane region (four out of six patterns of increase). Outside of the transmembrane region, only third-position transversions appeared to have diverged proportionally with DNA hybridization divergence. Griffiths (1997) discovered the same divergence patterns for bird of prey, although not for first-position transmembrane transitions. Sheldon, Whittingham, and Winkler (1999) found the same patterns for swallows, except for first- and second-position transmembrane transitions.

Graphs used to estimate Ti/Tv are shown in figure 5. When Ti/Tv is plotted against DNA hybridization distances (fig. 5*A*), not much pattern is evident. One high point on the left-hand side of the curve (Ti/Tv $\sim$ 24) is between two species (*E. tricolor* and *E. caerulea*) that differed by 50 transitions and only 2 transversions. When transitions per site are plotted against transversions per site (fig. 5*B*), the instantaneous Ti/Tv is about 6. Unfortunately, because most of the pairwise comparisons are intergeneric, there are relatively few points to define the initial slope of this curve. The Ti/Tv values estimated by maximum likelihood using the K3Puf + gamma model are 6.082/1 = 6.082 (for A$\leftrightarrow$C and G$\leftrightarrow$T) and 6.082/0.4858 = 12.52 (for A$\leftrightarrow$T and G$\leftrightarrow$C).

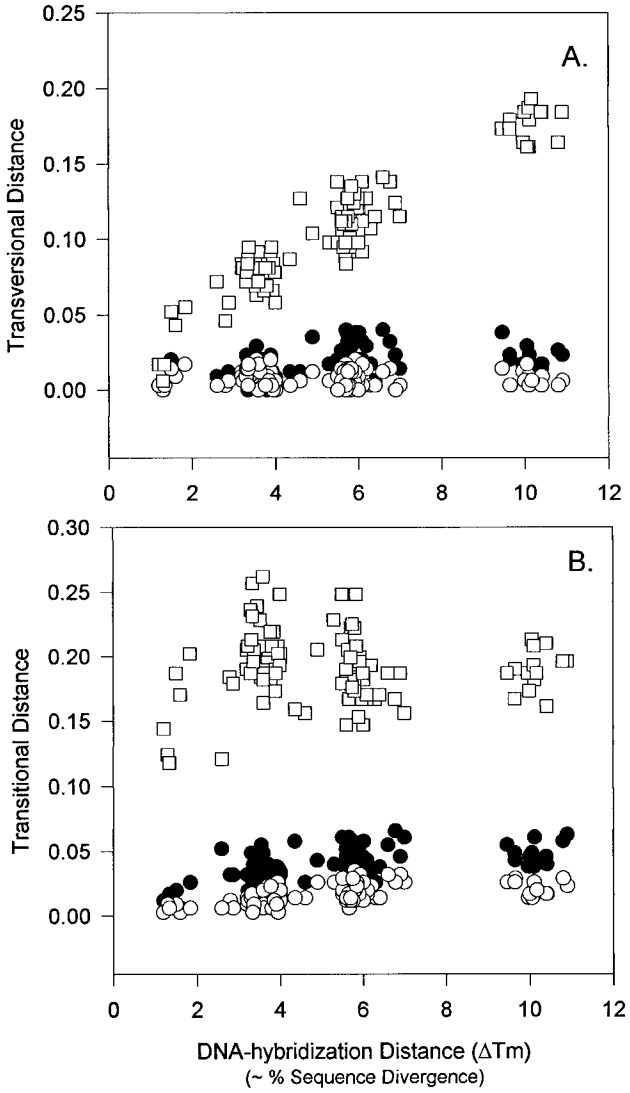

FIG. 3.—Uncorrected cytochrome *b* distances, partitioned as transversions and transitions and by codon site positions, versus DNA hybridization distances. *A*, Transversional distances. *B*, Transitional distances. Closed circles represent first-position distances, open circles represent second-position distances, and open squares represent third-position distances.

Estimates of Phylogeny

All phylogeny reconstruction methods (maximum likelihood, parsimony, and least-squares distance) based on data weighted a priori yielded trees similar in overall topology to the DNA hybridization tree (figs. 1*A* and 6): tiger heron (*Tigrisoma*) and boat-bill (*Cochlearius*) appear as basal lineages, and day and night herons form a distal clade, which is the sister group of the bitterns plus zigzag heron (*Zebrilus*). Within the day and night heron clade, support is consistent only for two groups: (*Syrigma*, (*E. thula, E. caerulea, E. tricolor*)) and ((*Ardea, Casmerodius*), *Bubulcus*). The relationship between these two groups, the night herons (*Nycticorax* and *Nyctanassa*), and green heron (*Butorides virescens*) is unresolved. The same is true in the DNA hybridization tree. Comparisons of the maximum-likelihood, most-parsimonious, and best distance trees using Kishino-Hasegawa tests of maximum-likelihood fits did not indicate a significant difference among the cytochrome *b* trees or between these trees and the DNA hybridization tree. Bootstrap analyses with Ti/Tv = 6.0 produced the tree in figure 6*D*. However, this tree appears overly conservative. Although it adequately summarizes the agreements and disagreements among the best trees, it collapses the branch separating the bitterns from the day and night herons. No other analysis, weighted or unweighted, indicates that any of the bitterns, or *Zebrilus*, belong in the day and night heron clade.

To attempt to improve resolution of the cytochrome *b* tree, we constructed trees from partitions of the data that appeared least saturated in figures 3 and 4 using unweighted parsimony. For example, the best tree inferred from third-position transversions had the same general structure as the best trees from complete data sets. Bootstrapping this partition using parsimony produced an unresolved tree, with only the following clades supported: (((*E. thula, E. caerulea* [85%]), *E. tricolor* [98%]), Syrigma [66%]); (*Bubulcus, Ardea, Casmerodius* [66%]); ((*Botaurus, Ixobrychus* [57%]), *Zebrilus* [54%]). We also tried to reconstruct trees using third-position transversions of the transmembrane and intermembrane regions. These data produced 26 most-parsimonious trees whose strict consensus was most similar to the topology in figure 6*A*. In general, analyses of partitions provided trees similar to those produced by weighted, complete data sets.

Lineage-Based Rates of Evolution

Comparisons of phenetic and patristic distances from the seven outgroups to all heron species by Friedman repeated-measures ANOVA indicated significant differences in distances between certain heron lineages. However, outgroup-to-ingroup distances differed depending on the type of distance measure. For example, when distance values were corrected using the K3Puf + gamma method, the tiger heron (*Tigrisoma*) distance was fairly long, the bittern (*Botaurus, Ixobrychus*, and *Zebrilus*) distances were not particularly long, and the *Egretta* distances were short. This pattern is evident in figures 6*A* and *C*. When distance values were derived solely from third-position transversions, the pattern of relative length changed dramatically: the tiger heron and boat-bill distances became significantly shorter than most other heron distances, and the egret and, especially, the bittern distances became longer. This pattern is evident in figure 7*A*.

Because the branch length pattern produced by third-position transversions (fig. 7*A*) resembled that of the DNA hybridization tree (figs. 1*A* and 7*B*), we tested the agreement of relative branch lengths in the two trees using Omland's (1994, 1997) total-evolution test (table 4). First, we chose a single topology consistent between the best cytochrome *b* and DNA hybridization trees. Many such trees are possible, given the lack of resolution in trees of both data sets. We selected the DNA hybridization topology because it represents the best tree

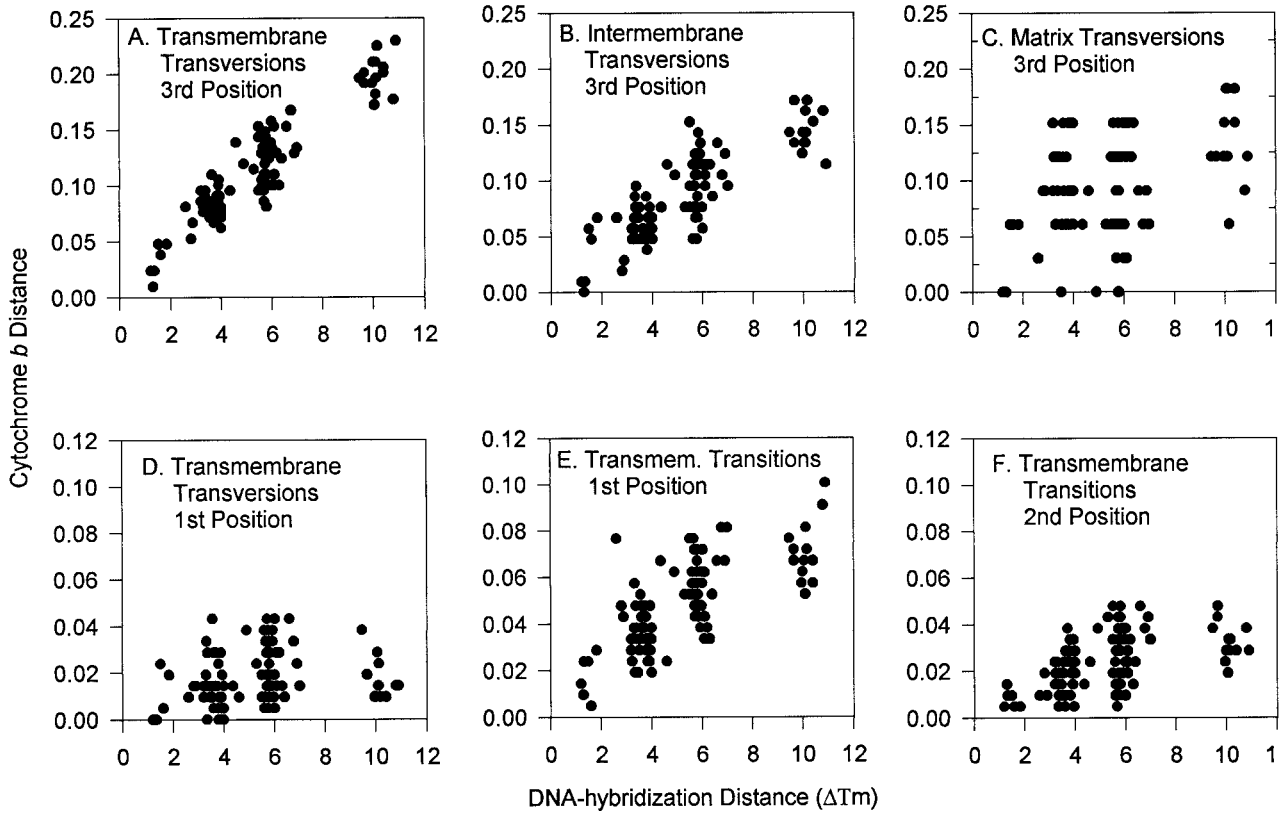

FIG. 4.—Distances computed for various cytochrome *b* protein regions versus DNA hybridization distances. Cytochrome *b* values are uncorrected proportional distances. Only those cytochrome *b* data partitions that increased with DNA hybridization distance are shown.

for these data and is very similar to the best cytochrome *b* trees (fig. 6). (When bootstrapping support is considered, the DNA hybridization and best cytochrome *b* topologies are completely congruent.) Then, we removed the zigzag heron (*Z. undulatus*) and tricolored heron (*E. tricolor*) from all data matrices, because we did not have a complete set of DNA hybridization comparisons for these two species. Third, we checked for a node density effect in the trees using the Spearman rank order method and found no correlation for the 13 nodes and branches: for DNA hybridization data $r_s = -0.122$ and $P = 0.682$; for unpartitioned cytochrome *b* data, $r_s = 0.130$ and $P = 0.629$; for cytochrome *b* third-position transversions, $r_s = 0.161$ and $P = 0.591$. Thus, we could use simple contrasts to test the relative branch length pattern, rather than contrasts corrected for a node density bias. Finally, we computed the DNA hybridization and cytochrome *b* contrasts from branch lengths produced by optimizing DNA hybridization distances and cytochrome *b* data on the DNA hybridization topology (table 4). For comparisons between DNA hybridization and unpartitioned cytochrome *b* data, 5 out of 12 contrasts agreed in sign (binomial test; $P = 0.613$). Between the DNA hybridization and cytochrome *b* third-position transversion data, 9 out of 12 contrasts agreed ($P = 0.073$). Given the stringency of this test (Omland 1997), these findings suggest substantial similarity in relative branch length patterns between the DNA hybridization and cytochrome *b* third-position transversion trees, but not between the DNA hybridization and unpartitioned cytochrome *b* data trees. This relationship is also evident in contrast correlations: for Spearman rank correlation between DNA hybridization and unpartitioned contrasts, $r_s = -0.116$ and $P = 0.696$, and between DNA hybridization and third-position transversion contrasts, $r_s = 0.660$ and $P = 0.013$.

Discussion

Heron Phylogeny

Herons have traditionally been divided into four or five ecological groups: day herons, night herons, bitterns, tiger herons, and boat-billed heron (Hancock and Kushlan 1984). Which species belong to which groups and how these groups are related to one another have been sources of endless speculation (e.g., Bock 1956; Curry-Lindahl 1971; Payne and Risley 1976; Sheldon 1987*b*). The only rigorous nonmolecular effort to reconstruct heron phylogeny, a cladistic analysis of osteological characters (Payne and Risley 1976), found a close relationship between day and tiger herons and (possibly) between boat-bill and night herons (fig. 1*B*). Similar arrangements of taxa have been argued by other morphologists (e.g., Bock 1956; Cracraft 1967). The morphological comparisons also indicated that whistling heron (*Syrigma*) is the sister group of day and tiger herons and that the cattle egret (*Bubulcus*) is closer to the true egrets (*Egretta*) than to the great blue heron (*Ardea*) and the great egret (*Casmerodius*). The scnDNA hybridization and cytochrome *b* sequence data, however,

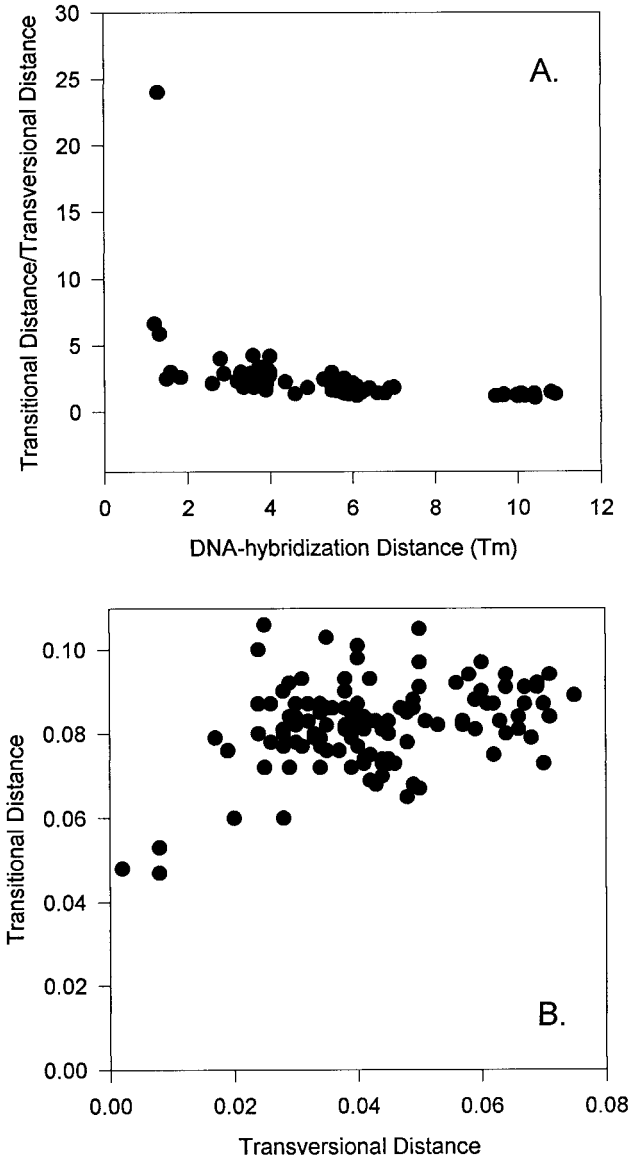

FIG. 5.—Alternative perspectives on the transition-to-transversion (Ti/Tv) relationship. *A,* Cytochrome *b* Ti/Tv values, based on uncorrected Ti and Tv distances, versus DNA hybridization distances. *B,* Cytochrome *b* distances based on transitions per site versus cytochrome *b* distances based on transversions per site.

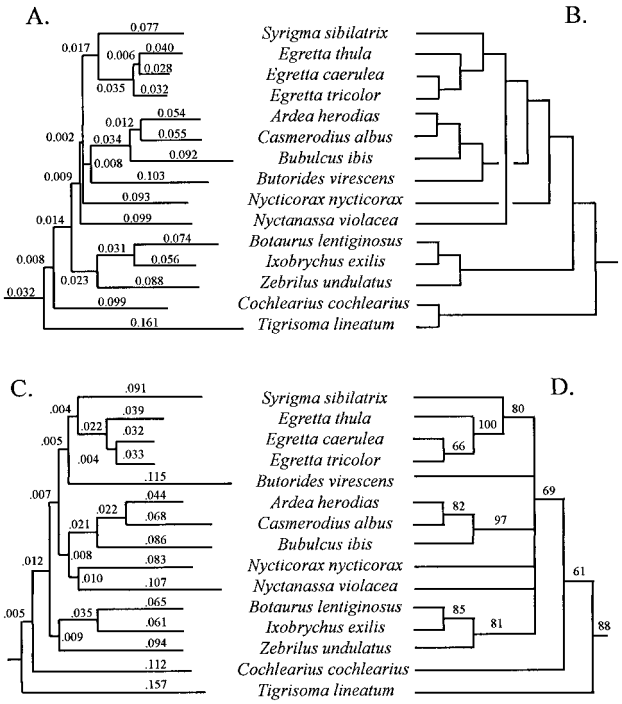

FIG. 6.—Cytochrome *b* trees. *A,* Maximum-likelihood tree from 20 randomized searches using the Kimura (1981) three-parameter model (general time- reversible rate factors: a and f = 1, b and e = 6.0821, c and d = 0.4858), with empirical base frequencies and gamma distribution rate adjustment ($\alpha = 0.2698$); lnL = −8,263.6458. *B,* Maximum-parsimony tree from 100 randomized heuristic searches, with the following weightings: Ti/Tv = 6; first : second : third codon site positions set at 3:3:1. Length = 5,319, consistency index = 0.597, retention index = 0.598. *C,* Least-squares tree using K3Puf + gamma ($\alpha = 0.26$) distances; sum of squares = 0.138. *D,* Fifty percent majority-rule consensus tree of 100 replicated bootstraps (10 random searches each) using parsimony with a Ti/Tv ratio of 6. The outgroups for all trees (not shown) were *Plegadis falcinellus, Scopus umbretta, Platalea alba, Balaeniceps rex, Coragyps atratus, Mycteria americana,* and *Gallus domesticus.*

support a substantially different phylogeny (figs. 1*A,* 6, and 7) from that supported by the morphological data (fig. 1*B*). The molecular data indicate that (1) day and night herons form a clade, (2) tiger herons and boat-billed heron branch from the base of the heron tree, (3) *Syrigma* belongs in the egret clade, and (4) *Bubulcus* is part of the *Ardea-Casmerodius* clade. The agreement between these independent molecular data sets provides strong corroborative evidence of the basic structure of heron phylogeny (Bledsoe and Raikow 1990; McCracken and Sheldon 1998). This is particularly true if one considers that scnDNA hybridization and cytochrome *b* gene data represent unlinked genomes and were subjected to largely different methods of analysis (distance vs. parsimony and maximum likelihood). The overall congruence of the molecular data puts to rest long-standing questions about higher-level relationships of herons.

Unfortunately, because of poor resolution in parts of the cytochrome *b* and DNA hybridization trees, we are not able to answer some other questions about heron relationships. With the exception of the interrelationship among great blue herons (*Ardea herodias*), great egrets (*Casmerodius albus*), and cattle egrets (*Bubulcus ibis*), the cytochrome *b* sequence data did not clarify branching positions within clades. Within the large clade consisting of day and night herons, for example, relationships among the main groups remain unclear. It is not even certain whether the night herons are monophyletic. Similarly, at the basal end of the heron tree, it is not clear whether boat-billed (*Cochlearius*) and tiger herons (*Tigrisoma*) are sister taxa or consecutive outgroups. The cytochrome *b* analyses suggest that the tiger heron is the outgroup to the other herons, but this positioning does not hold up particularly well to bootstrapping (61% support; fig. 6*D*). DNA hybridization might have solved this problem, except that two DNA hybridization studies yielded different topologies for the lineages deriving at the base of the heron tree. In Sheldon (1987*b*), tiger

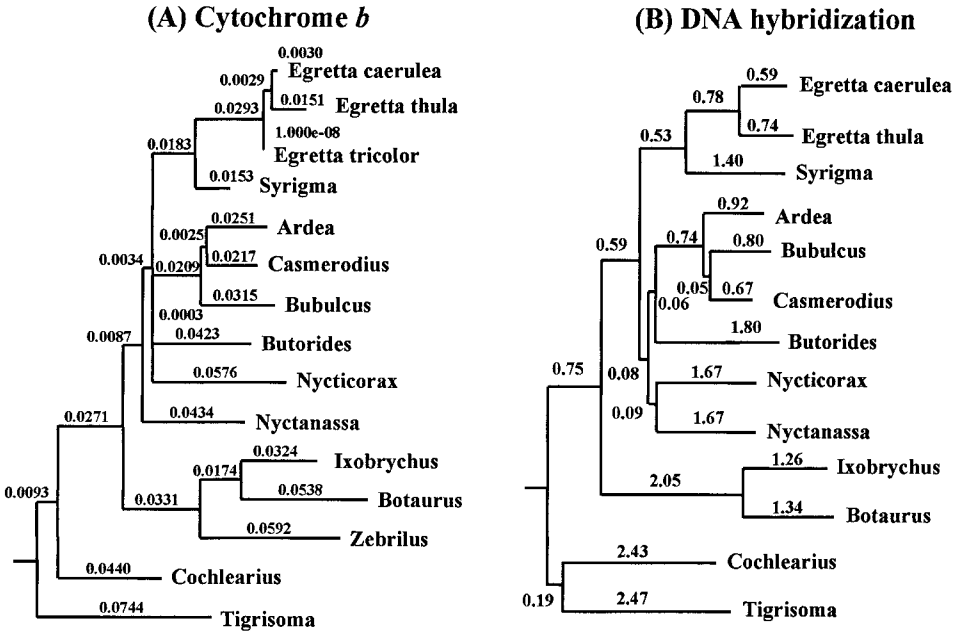

FIG. 7.—Comparison of cytochrome *b* and DNA hybridization branch lengths when cytochrome *b* data are limited to third-position transversions. *A*, Cytochrome *b* tree topology from figure 6*A*, in which branch lengths were determined by maximum-likelihood optimization using third-position transversions. Base pairs were coded as either purines or pyrimidines, and first and second positions were removed; lnL = −1,892.09733, estimated $\alpha = 0.539$. *B*, Best DNA hybridization tree built from the distances in Sheldon (1987*b*) using unweighted least-squares (PHYLIP, Fitch program; Felsenstein 1995); sum of squares = 3.80. This DNA hybridization tree topology was used in the Omland (1994, 1997) test of lineage-based rates.

herons and boat-billed heron were supported as sister taxa by jackknife analysis. In Sheldon, McCracken, and Stuebing (1995), two more tiger heron species were added to the matrix, and bootstrap analysis supported tiger herons as the outgroup to all other herons, including boat-billed heron. However, in this latter study, only four species were used to represent the other heron clades. Thus, in both of the DNA hybridization studies, taxon sampling was inadequate. To reflect this uncertainty in the DNA hybridization results, we represented the tiger heron and boat-billed heron relationships as a multifurcation (fig. 1*A*). Except for the *Ardea*, *Casmerodius*, and *Bubulcus* case mentioned above, the unresolved DNA hybridization tree (fig. 1*A*) still represents the best estimate of heron phylogeny, even after the cytochrome *b* analyses presented here.

Table 4
Data for the Omland (1997) Total-Evolution Test of Branch Length Correlation Between DNA Hybridization and Cytochrome *b* Trees

			ΔTm		Cytochrome *b*, All Data		Cytochrome *b*, Third-Position Transversions	
Taxa[a]	Contrast Code[b]	No. of Nodes[c]	Branch	Contrast	Branch	Contrast	Branch	Contrast
Casmerodius (C)		6	2.94		0.152		0.087	
Bubulcus (B)	C-B	6	3.07	−0.13	0.198	−0.046	0.096	−0.009
Ardea (A)	CB-A	5	3.14	−0.135	0.151	0.024	0.090	0.0015
Butorides (B)	CBA-B	4	3.28	−0.2075	0.155	0.008	0.084	0.00675
Nyctanassa (N)	N-N	4	3.179	−0.001	0.151	0.012	0.089	−0.014
Nycticorax (N)	CBAB-NN	4	3.18	−0.00325	0.139	0.014	0.103	−0.00863
Egretta caerulea (E)	E-E	4	3.24	−0.15	0.114	−0.007	0.096	−0.014
Egretta thula (E)	EE-S	4	3.39	0.045	0.121	−0.0145	0.110	0.024
Syrigma (S)	CBABNN-EES	3	3.27	−0.11462	0.132	0.02725	0.079	0.000688
Ixobrychus (I)	I-B	2	4.06	−0.08	0.150	−0.014	0.115	−0.005
Botaurus (B)	CBABNNEES-IB	2	4.14	−0.86481	0.164	−0.01863	0.120	−0.02616
Cochlearius (C)	C-T	1	2.62	−0.04	0.114	−0.099	0.042	−0.041
Tigrisoma (T)	CBABNNEESIB-CT	1	2.66	1.027594	0.213	−0.01581	0.083	0.041922

[a] For this test, the DNA hybridization topology (fig. 7*B*) was used, and the contrasts were computed from the top to the bottom of the tree, starting with *Casmerodius* and following the order in the ''taxa'' column.

[b] The ''contrast code'' column shows the order of contrast computations. For example, C-B = total *Casmerodius* lineage length (from ingroup node to branch tip) minus total *Bubulcus* lineage length. Another example: CBA-B = ((C + B)/2 + A)/2 − B, where the first B refers to *Bubulcus* lineage length and the second B refers to *Butorides* lineage length.

[c] The number of nodes is counted from (but does not include) the ingroup node.

The reason for the lack of resolution within the day and night heron clade and at the base of the heron tree is unclear. Resolution may be difficult (or impossible) simply because the unresolved nodes are too closely spaced in time to be teased apart. However, tightly spaced divergence dates may not explain the whole problem; limitations in the two molecular data sets appear to have contributed uncertainty as well. DNA hybridization cannot resolve close branching points in bird trees because of its substantial measurement error (± ΔTm 0.2 for herons; Sheldon 1987*b*) combined with the relatively slow rate of bird scnDNA evolution. Indeed, one reason we repeated the phylogenetic analysis of herons using the cytochrome *b* gene was to take advantage of that gene's relatively fast rate of evolution and supposed ability to resolve relationships among closely related taxa (Moore and DeFilippis 1997). However, the evolutionary rate of the cytochrome *b* gene appears to have been too fast in most cases. Virtually the only cytochrome *b* data that were resilient to bootstrapping involved divergence values below 11%, i.e., unsaturated data (fig. 2). This divergence range was limited to species within the *Egretta-Syrigma, Ardea-Casmerodius-Bubulcus,* and bittern-*Zebrilus* clades (fig. 6*D*). Although we identified partitions of the cytochrome *b* gene sequence that had the potential to resolve more distant relationships (e.g., third-position transversions), these data appeared to be too few to stand up to bootstrapping when used by themselves or when weighted heavily and used in conjunction with the rest of the sequence data.

Measures of Relative Time

In the absence of absolute divergence dates, DNA hybridization distances were used in graphs to provide a perspective of cytochrome *b* sequence change over relative time (figs. 2–5). Usually, relative time is represented on the x-axis by total (unpartitioned) sequence distances corrected for back mutations (e.g., Hackett 1996; Griffiths 1997). That the two approaches to estimating relative time—DNA hybridization distance and corrected total sequence divergence—yield different perspectives on patterns of sequence change is apparent when figure 3*A* is compared with figure 8. Figure 3*A* depicts third-position transversional distances plotted against DNA hybridization distances; figure 8 depicts third-position transversional distances plotted against total cytochrome *b* distances that have been corrected for back mutations by the K3Puf and K3Puf + gamma methods, respectively.

The distances in the Kimura three-parameter plots (fig. 8) are either tightly packed into an upward curve (K3Puf distances) or relatively scattered (K3Puf + gamma distances). The truncation of the K3Puf plot in figure 8 indicates that the complete sequence (unpartitioned) distances suffer not only more saturation than the DNA hybridization distances, but also more saturation than third-position transversions. (The saturation of corrected cytochrome *b* distances is also evident in fig. 2.) The scatter (but improved linearity) of the K3Puf + gamma distances is caused by the addition of another parameter

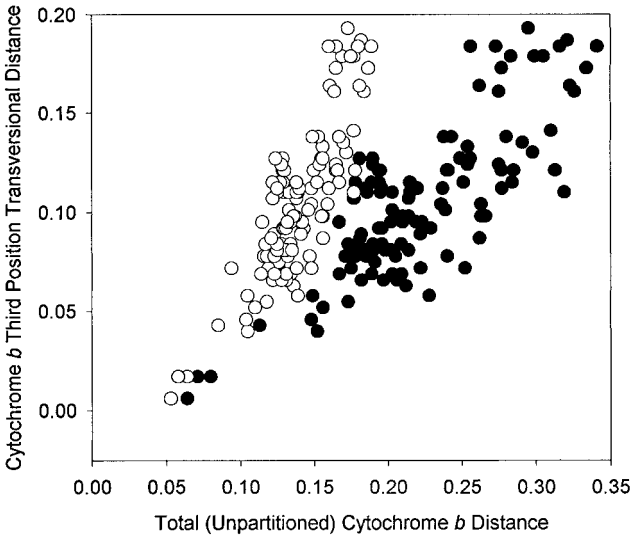

FIG. 8.—Distances based on cytochrome *b* third-position transversions versus distances from total (unpartitioned) cytochrome *b* data corrected by the K3Puf method (open circles) and by the K3Puf + gamma method (closed circles).

to the distance model. Variance is expected to increase with the addition of parameters. This is why it is desirable to use a distance or maximum-likelihood model with as few parameters as possible (Swofford et al. 1996; Posada and Crandall 1998).

In comparison with the plots in figure 8, the DNA hybridization plot (fig. 3*A*) displays more linearity and less variance. It also exhibits fairly distinct clusters of points. These clusters—e.g., at ΔTm ≈ 1–2, 2.5, 3.5–4, 6, and 10—reflect primarily distances among species in separate, major clades. The most obvious and consistent set of such distances is between ingroup and outgroup members (herons to ibis, ΔTm ~ 10). In figure 8, clusters of distances are evident only between ingroup and outgroup members and among the least diverged taxa. Other clusters are obscured by either compression of distances (K3Puf plot) or scatter (K3Puf + gamma plot) or both. The scatter in the K3Puf + gamma plot is a result of the small sample size inherent in cytochrome *b* sequences (1,041 bases); were the sequences longer, it would have been reduced. Conversely, the relative lack of scatter in the DNA hybridization plot is due to the fact that DNA hybridization distances are based on the comparison of tens of thousands, if not millions, of base pairs.

Rates of Evolution

Perhaps the most interesting discovery of our analysis is that heron nuclear and mitochondrial DNAs display similar underlying lineage-based rates of evolution. This discovery adds to a growing body of evidence to this effect. Martin (1999) discovered the same phenomenon when he compared shark trees inferred from nuclear RAG-1 and mitochondrial cytochrome *b* genes. Mindell et al. (1996) found that nuclear and mitochondrial protein-coding genes have evolved, in general, more slowly in chickens (*Gallus gallus*) than in repre-

sentative mammals (*Homo sapiens*, *Mus musculus*, and *Rattus novegicus*). Preliminary molecular comparisons of tubenosed birds (Procellariiformes) suggest that both scnDNA and the cytochrome *b* gene evolve more slowly in clades consisting of large-bodied, as opposed to small-bodied, species (Sibley and Ahlquist 1990; Nunn and Stanley 1998). Similar results have been found in comparisons of mammalian orders consisting mainly of large- versus small-bodied species (Martin and Palumbi 1993).

A variety of causes have been suggested to account for molecular rate variation, including differences in metabolic rate, generation time, rate of germ cell division, body temperature, DNA repair efficiency, population sizes, and clade size (reviewed by Martin and Palumbi 1993; Rand 1994; Omland 1997; Bleiweiss 1998). For herons, we lack data on most of these suspected causes. However, because several of the potential causes, such as metabolic rate and generation time, are correlated with body size (Martin and Palumbi 1993; Bleiweiss 1998), we can look for a relationship between body size and molecular rate as an approximate indicator of cause. A quick examination of the herons, however, reveals that body size does not explain their molecular rate pattern. For example, the fast-evolving bitterns include of some of the largest (*Botaurus* spp.) as well as some of the smallest (*Ixobrychus* spp.) heron species. Another potential cause of rate variation, clade size, is also easily examined for the herons. Speciose clades are expected to exhibit faster rates of molecular evolution than depauperate clades because of the genetic sampling phenomena (drift, bottlenecks, etc.) and potential ''genetic revolutions'' (Mayr 1963) associated with speciation (Omland 1997). A relationship between evolutionary and speciation rates has been proposed many times based on taxonomic patterns (e.g., Eldredge and Gould 1972) and genetic studies (e.g., Nichol, Rowe, and Fitch 1993; Barraclough, Harvey, and Nee 1996; Moran 1996). In herons, the most speciose clades—bitterns (12 species of *Botaurus* and *Ixobrychus*) and true egrets (11 species of *Egretta*)—appear to have evolved the fastest. Conversely, depauperate clades—tiger herons (five species) and boat-billed heron (1 species)—appear to have evolved slowly. Unfortunately, this rate–to–clade size relationship is difficult to quantify in herons because, even if we had sampled all of the species, there would not have been enough clades exhibiting alternative species numbers and rates to test repetitive patterns by comparative methods. Moreover, we have no idea of the historical diversity of heron clades (i.e., how much extinction they have experienced).

A simple causal explanation for rate variation in birds remains elusive, in part because of a dearth of data, but also because different groups may have been influenced by different forces. In an unusually careful demonstration, Bleiweiss (1998) found that lineage-based rates of scnDNA evolution in hummingbirds are correlated with metabolic rates, but Mindell et al. (1996) argued that metabolism could not be responsible for rate differences between birds and mammals based on comparisons of nuclear and mitochondrial protein-coding and ribosomal genes. These two studies compared taxa on very different hierarchical levels, and patterns observed between classes of vertebrates may not be expected to occur within classes. Moreover, even within the class Aves, rates of molecular evolution in different orders could be influenced by different factors. One would predict, for example, that metabolism should be an important force in the evolution of hummingbirds (Rand 1994), but metabolism seems less likely to be important in herons and tubenoses. As we gather more data on rates of evolution in closely related birds, the accuracy of these predictions should be revealed.

Acknowledgments

We thank the following institutions for help in obtaining tissues for this study: the Academy of Natural Sciences of Philadelphia, the LSU Museum of Natural Science, and the Yale Peabody Museum. For comments on the manuscript, we thank Beth Stewart and Peter Houde. John Harshman suggested we use Omland's (1994, 1997) test, and K. Naoki helped with statistics. This research was supported by NSF grants BSR-8806890, BSR-9020183, BSR-9207981, and NSF/LaSER 1993-96-ADP-02.

LITERATURE CITED

AVISE, J. C. 1994. Molecular markers, natural history, and evolution. Chapman and Hall, New York.

BARRACLOUGH, T. G., P. H. HARVEY, and S. NEE. 1996. Rate of *rbc*L gene sequence evolution and species diversification in flowering plants (angiosperms). Proc. R. Soc. Lond. B Biol. Sci. **263**:589–591.

BLEDSOE, A. H., and R. J. RAIKOW. 1990. A quantitative assessment of congruence between molecular and nonmolecular estimates of phylogeny. J. Mol. Evol. **30**:247–259.

BLEIWEISS, R. 1998. Relative-rate tests and biological causes of molecular evolution in hummingbirds. Mol. Biol. Evol. **15**:481–491.

BLEIWEISS, R., and J. A. W. KIRSCH. 1992. Experimental analysis of variance for DNA hybridization: I. Accuracy. J. Mol. Evol. **37**:504–513.

BOCK, W. J. 1956. A generic review of the family Ardeidae (Aves). Am. Mus. Novit. **1779**:1–49.

BRITTEN, R. J., D. E. GRAHAM, and B. R. NEUFELD. 1974. Analysis of repeating DNA sequences by reassociation. P. 363 *in* L. GROSSMAN and K. MOLDAVE, eds. Methods in enzymology. Vol. 29. Academic Press, New York.

BROWN, W. M., M. GEORGE, and A. C. WILSON. 1979. Rapid evolution of animal mitochondrial DNA. Proc. Natl. Acad. Sci. USA **76**:1967–1971.

CRACRAFT, J. 1967. On the systematic position of the boat-billed heron. Auk **84**:529–533.

CURRY-LINDAHL, K. 1971. Systematic relationships in herons (Ardeidae), based on comparative studies of behavior and ecology. Ostrich Suppl. **9**:53–70.

DEGLI ESPOSTI, M., S. DE VRIES, M. CRIMI, A. GHELLI, T. PATARNELLO, and A. MEYER. 1993. Mitochondrial cytochrome *b*: evolution and structure of the protein. Biochem. Biophys. Acta **1143**:243–271.

DESJARDINS, P., and R. MORAIS. 1990. Sequence and gene organization of the chicken mitochondrial genome. A novel gene order in higher vertebrates. J. Mol. Biol. **212**:599–634.

EDWARDS, S. V. 1997. Relevance of microevolutionary processes to higher level molecular systematics. Pp. 251–278 *in* D. P. MINDELL, ed. Avian molecular evolution and systematics. Academic Press, New York.

EDWARDS, S. V., P. ARCTANDER, and A. C. WILSON. 1991. Mitochondrial resolution of a deep branch in the genealogical tree for perching birds. Proc. R. Soc. Lond. B Biol. Sci. **243**:99–107.

ELDREDGE, N., and S. J. GOULD. 1972. Punctuated equilibria: an alternative to phyletic gradualisms. Pp. 82–115 *in* T. J. M. SCHOPF, ed. Models in paleobiology. Freeman, Cooper, and Co., San Francisco.

FELSENSTEIN, J. 1984. Distance methods for inferring phylogenies: a justification. Evolution **38**:16–24.

———. 1989. PHYLIP—phylogeny inference package (version 3.2). Cladistics **5**:164–166.

———. 1995. PHYLIP—phylogenetic inference package. Version 3.5c. Distributed by the author, Department of Genetics, University of Washington, Seattle.

FITCH, W. M., and M. BRUSCHI. 1987. The evolution of prokaryotic ferredoxins—with a general method correcting for unobserved substitutions in less branched lineages. Mol. Biol. Evol. **4**:381–394.

GRIFFITHS, C. S. 1997. Correlation of functional domains and rates of nucleotide substitution in cytochrome *b*. Mol. Phylogenet. Evol. **7**:352–365.

HACKETT, S. J. 1996. Molecular phylogenetics and biogeography of tanagers in the genus *Ramphocelus* (Aves). Mol. Phylogenet. Evol. **5**:368–382.

HANCOCK, J., and J. KUSHLAN. 1984. The herons handbook. Harper and Row, New York.

HASEGAWA, M., H. KISHINO, and T. YANO. 1985. Dating of the human-ape splitting by a molecular clock of mitochondrial DNA. J. Mol. Evol. **22**:160–174.

HELM-BYCHOWSKI, K., and J. CRACRAFT. 1993. Recovering phylogenetic signal from DNA sequences; relationships within the corvine assemblage (class Aves) as inferred from complete sequences of the mitochondrial DNA cytochrome *b* gene. Mol. Biol. Evol. **10**:1196–1214.

HILLIS, D. M., A. LARSON, S. K. DAVIS, and E. A. ZIMMER. 1990. Nucleic acids III; sequencing. Pp. 318–370 *in* D. M. HILLIS and C. MORITZ, eds. Molecular systematics. Sinauer, Sunderland, Mass.

HOUDE, P. 1987. Critical evaluation of DNA hybridization studies in avian systematics. Auk **104**:17–32.

IRWIN, D. M., T. D. KOCHER, and A. C. WILSON. 1991. Evolution of the cytochrome *b* gene of mammals. J. Mol. Evol. **32**:128–144.

KIMURA, M. 1981. Estimation of evolutionary distances between homologous nucleotide sequences. Proc. Natl. Acad. Sci. USA **78**:454–458.

KISHINO, H., and M. HASEGAWA. 1989. Evaluation of the maximum likelihood estimate of the evolutionary tree topologies from DNA sequence data, and the branching order in Hominoidea. J. Mol. Evol. **29**:170–179.

KOCHER, T. D., W. K. THOMAS, A. MEYER, S. V. EDWARDS, S. PAABO, F. X. VILLABLANCA, and A. C. WILSON. 1989. Dynamics of mitochondrial DNA evolution in animals: amplification and sequencing with conserved primers. Proc. Natl. Acad. Sci. USA **86**:6196–6200.

KUMAR, S., K. TAMURA, and M. NEI. 1993. MEGA: molecular evolutionary genetics analysis. Version 1.01. The Pennsylvania State University, University Park.

MCCRACKEN, K. G., and F. H. SHELDON. 1998. Molecular and osteological heron phylogenies: sources of incongruence. Auk **115**:127–141.

MADDISON, W. P., and D. R. MADDISON. 1992. MacClade: analysis of phylogeny and character evolution. Version 3.0. Sinauer, Sunderland, Mass.

MARTIN, A. P. 1999. Substitution rates of organelle and nuclear genes in sharks: implicating metabolic rate (again). Mol. Biol. Evol. **16**:996–1002.

MARTIN, A. P., and S. R. PALUMBI. 1993. Body size, metabolic rate, generation time, and the molecular clock. Proc. Natl. Acad. Sci. USA **90**:4087–4091.

MAYR, E. 1963. Animal species and evolution. Belknap Press, Cambridge, Mass.

MINDELL, D. P., A. KNIGHT, C. BAER, and C. J. HUDDLESTON. 1996. Slow rates of molecular evolution in birds and the metabolic rate and body temperature hypotheses. Mol. Biol. Evol. **13**:422–426.

MOORE, W. S., and V. R. DEFILIPPIS. 1997. The window of taxonomic resolution for phylogenies based on mitochondrial cytochrome *b*. Pp. 83–119 *in* D. P. MINDELL, ed. Avian molecular evolution and systematics. Academic Press, New York.

MORAN, N. A. 1996. Accelerated evolution and Muller's rachet in endosymbiotic bacteria. Proc. Natl. Acad. Sci. USA **93**: 2873–2878.

NICHOL, S. T., J. E. ROWE, and W. FITCH. 1993. Punctuated equilibrium and positive Darwinian evolution in vesicular stomatitis virus. Proc. Natl. Acad. Sci. USA **90**:10424–10428.

NUNN, G. B., and J. CRACRAFT. 1996. Phylogenetic relationships among the major lineages of the birds-of-paradise (Paradisaeidae) using mitochondrial gene sequences. Mol. Phylogenet. Evol. **5**:445–459.

NUNN, G. B., and S. E. STANLEY. 1998. Body size effects and rates of cytochrome *b* evolution in tube-nosed seabirds. Mol. Biol. Evol. **15**:1360–1371.

OMLAND, K. E. 1994. Character congruence between a molecular and a morphological phylogeny for dabbling ducks (*Anas*). Syst. Biol. **43**:369–386.

———. 1997. Correlated rates of molecular and morphological evolution. Evolution **5**:1381–1393.

PAYNE, R. B., and C. J. RISLEY. 1976. Systematics and evolutionary relationships among the herons (Ardeidae). Misc. Publ. Univ. Mich. Mus. Zool. **150**:1–115.

POSADA, D., and K. A. CRANDALL. 1998. MODELTEST: testing the model of DNA substitution. **14**:817–818.

QUINN, T. W. 1997. Molecular evolution of the mitochondrial genome. Pp. 3–28 *in* D. P. MINDELL, ed. Avian molecular evolution and systematics. Academic Press, New York.

RAND, D. M. 1994. Thermal habit, metabolic rate, and the evolution of mitochondrial DNA. Trends Ecol. Evol. **9**:125–130.

SANGER, F. S., S. NICKLEN, and A. R. COULSON. 1977. DNA sequencing with chain-terminating inhibitors. Proc. Natl. Acad. Sci. USA **74**:5463–5467.

SARICH, V. M., and A. C. WILSON. 1967. Immunological time scale for hominoid evolution. Science **158**:1200–1203.

SHELDON, F. H. 1987*a*. Rates of single-copy DNA evolution in herons. Mol. Biol. Evol. **4**:56–69.

———. 1987*b*. Phylogeny of herons estimated from DNA-DNA hybridization data. Auk **104**:97–108.

SHELDON, F. H., and A. H. BLEDSOE. 1989. Indexes to the reassociation and stability of solution DNA hybrids. J. Mol. Evol. **29**:328–343.

SHELDON, F. H., and M. KINNARNEY. 1993. The effect of sequence removal on DNA hybridization estimates of distance, phylogeny, and rates of evolution. Syst. Biol. **42**:32–48.

SHELDON, F. H., K. G. MCCRACKEN, and K. D. STUEBING. 1995. Phylogenetic relationships of the zigzag heron (*Zebrilus undulatus*) and white-crested bittern (*Tigriornis leucolophus*) estimated by DNA-DNA hybridization. Auk **112**: 672–679.

SHELDON, F. H., L. A. WHITTINGHAM, and D. W. WINKLER. 1999. A comparison of cytochrome *b* and DNA hybridization data bearing on the phylogeny of swallows (Aves: Hirundinidae). Mol. Phylogenet. Evol. **11**:320–331.

SIBLEY, C. G., and J. E. AHLQUIST. 1990. Phylogeny and classification of birds. Yale University Press, New Haven, Conn.

SLIKAS, B. 1997. Phylogeny of the avian family Ciconiidae (storks) based on cytochrome *b* sequences and DNA-DNA hybridization distances. Mol. Phylogenet. Evol. **8**:275–300.

SORENSON, M. D., and R. C. FLEISCHER. 1996. Multiple independent transpositions of mitochondrial DNA control region sequences to the nucleus. Proc. Natl. Acad. Sci. USA **93**:15239–15243.

SORHANNUS, U., and C. VAN BELL. 1999. Testing for equality of molecular evolutionary rates: a comparison between a relative-rate test and a likelihood ratio test. Mol. Biol. Evol. **16**:849–855.

SPRINGER, M. S., E. H. DAVIDSON, and R. J. BRITTEN. 1992. Calculation of sequence divergence from the thermal stability of DNA heteroduplexes. J. Mol. Evol. **34**:379–382.

SWOFFORD, D. L. 1998. PAUP*. Phylogenetic analysis using parsimony (*and other methods). Version 4. Sinauer, Sunderland, Mass.

SWOFFORD, D. L., G. J. OLSEN, P. J. WADDELL, and D. M. HILLIS. 1996. Phylogenetic inference. Pp. 407–514 *in* D. M. HILLIS, C. MORITZ, and B. K. MABLE, eds. Molecular evolution. Sinauer, Sunderland, Mass.

ZHANG, Z., L. HUANG, V. M. SHULMEISTER, Y.-I. CHI, K. K. KIM, L.-W. HUNG, A. R. CROFTS, E. A. BERRY, and S.-H. KIM. 1998. Electron transfer by domain movement in cytochrome bc_1. Nature **392**:677–684.

CARO-BETH STEWART, reviewing editor

Accepted November 18, 1999